

Experimental study on the compression of concrete filled steel tubular latticed columns with variable cross section

Yan Yang^{*1}, Jun Zhou^{1a}, Jiangang Wei^{1b},
Lei Huang^{2c}, Qingxiong Wu^{1d} and Baochun Chen^{1e}

¹ College of Civil Engineering, Fuzhou University, Fuzhou 350116, China

² College of Civil Engineering and Architecture, Wuyi University, Nanping 354300, China

(Received May 06, 2016, Revised September 19, 2016, Accepted October 20, 2016)

Abstract. The effects of slenderness ratio, eccentricity and column slope on the load-carrying capacities and failure modes of variable and uniform concrete filled steel tubular (CFST) latticed columns under axial and eccentric compression were investigated and compared in this study. The results clearly show that all the CFST latticed columns with variable cross section exhibit an overall failure, which is similar to that of CFST latticed columns with a uniform cross section. The load-carrying capacity decreases with the increase of the slenderness ratio or the eccentricity. For 2-m specimens with a slenderness ratio of 9, the ultimate load-carrying capacity is increased by 3% and 5% for variable CFST latticed columns with a slope of 1:40 and 1:20 as compared with that of uniform CFST latticed columns, respectively. For the eccentrically compressed variable CFST latticed columns, the strain of the columns at the loading side, as well as the difference in the strain, increases from the bottom to the cap, and a more significant increase in strain is observed in the cross section closer to the column cap.

Keywords: concrete filled steel tubular latticed columns; axial compression; eccentric compression; stress mechanism; failure mode; load-carrying capacity

1. Introduction

Most piers of concrete filled steel tubular (CFST) bridge are columnar piers, according to the section forms of piers; it can be roughly divided into two categories, namely single-column piers and multiple-column piers, among of them, multiple-column piers consisting of two or more CFST latticed columns with either a variable cross section or a uniform cross section. However, as compared with those CFST latticed columns with a uniform cross section (hereafter referred to as “uniform CFST latticed columns”), CFST latticed columns with a variable cross section (hereafter referred to as “variable CFST latticed columns”) appear to have better mechanical properties and a more attractive appearance. More importantly, the stability of variable CFST latticed columns can

*Corresponding author, Assistant Professor, E-mail: yangyan@fzu.edu.cn

^a Ph.D. Student, E-mail: 329586362@qq.com

^b Professor, E-mail: weijg@fzu.edu.cn

^c Assistant, E-mail: 262036316@qq.com

^d Professor, E-mail: wuqingx@fzu.edu.cn

^e Professor, E-mail: baochunchen@fzu.edu.cn

be significantly improved due to the lowering of the center of gravity. Variable CFST latticed columns also perform well in absorbing and dissipating seismic energy, thus reducing the seismic response in areas vulnerable to high-magnitude earthquakes. All of these advantages make variable CFST latticed columns particularly appealing for applications in bridge piers, factory buildings, large-span CFST truss arches, high-rise buildings, equipment support frames, towers for power transmission, etc.

A number of theoretical studies have been performed on the compressed members with a variable cross section (Bleich 1952, Lee *et al.* 1981). The development of simulation techniques in recent years makes it possible to examine the effects of various geometric parameters on the load-carrying capacity of members with a variable cross section under different constraint conditions, and then these geometric parameters are corrected based on the numerical simulation results and more accurate formulas can be obtained for the design and construction of variable cross sectional members (Paul 1995, An *et al.* 2012) and mono-symmetric cross sectional members (Mohri *et al.* 2013). Nonlinear elastic-plastic analysis and experimental tests have been performed on tapered beam-columns subjected to both bending moment and compressive axial force (Han *et al.* 2011, Cristutiu and Dogariu 2012, Xue *et al.* 2014, Qu *et al.* 2015). Stability of steel frames with variable cross-section were also analyzed (Samofalov and Šlivinskas 2009). Parameter analysis has also been performed to determine the elastic buckling load and the ultimate load-carrying capacity of latticed columns using both experimental and finite element approaches (Mijailovic 2010, Razdolsky 2011, Dai *et al.* 2013 and Banan and Fouladi 2015).

Some scholars have experimentally investigated the effect of slenderness ratio and eccentricity on the load-carrying capacity of uniform CFST latticed columns under axial and eccentric compression (Jiang *et al.* 2011, Ou *et al.* 2011 and Shi *et al.* 2012), and some other studies have focused on the mechanical properties of solid columns with a variable cross section (Li and Li 2004). However, we are not aware of any study that has addressed the load-carrying capacities of variable CFST latticed columns. To address this problem, we compared the load-bearing capacities and failure modes between variable CFST latticed columns and uniform CFST latticed columns under axial and eccentric compression. In addition, we also investigated the effects of slenderness ratio, eccentricity and column slope on the load-carrying capacities of variable CFST latticed columns.

2. Presentation of the experiment

2.1 Specimens and material properties

A total of 8 specimens, each consisting of four CFST latticed columns connected by lacing tubes, were constructed, including 2 specimens with a uniform cross section and 6 specimens with a variable cross section. The parameters in this study included slenderness ratio, eccentricity and column slope, which were determined according to the loading conditions that could be provided in the laboratory and the requirements of practical applications (Dai *et al.* 2013) and China Association for Engineering Construction Standardization, Specification for Design and Construction of Concrete Filled Steel Tubular Structures (Code). In this study, the column height is 2 m or 3.5 m, the slenderness ratio is 13 or 23, the eccentricity is 0–0.12 m, and the slope is 1:40 or 1:20, respectively, as shown in Table 1.

For variable CFST latticed columns, the spacing between two columns in the in-plane direction is increased from the top of column to the bottom of column bottom at a fixed slope of 1:20 or

Table 1 Parameter and test results of specimens

No.	Types of lacing tubes	Column height <i>l</i> (m)	Slenderness ratio	Column slope 1 : <i>n</i>	Eccentricity (m)	Ultimate load-carrying capacity <i>N_u</i> (kN)
PH1		2.0	13	/	0	2173
PH2		3.5	23	/	0	2089
PH1-1	Horizontal lacing tubes	2.0	13	1 : 40	0	2236
PH1-2		2.0	13	1 : 20	0	2288
PH2-1		3.5	23	1 : 40	0	2138
PH2-2		3.5	23	1 : 20	0	2149
PH1-1-1		2.0	13	1 : 40	0.06	1635
PH1-1-2		2.0	13	1 : 40	0.12	1322

Note: In the naming of specimens, P = horizontal lacing tubes; H1: column height = 2 m, H2: column height = 3.5 m; The number after the first hyphen, 1: column slope = 1: 40, 2: column slope = 1: 20; The number after the second hyphen, no number: axial compression, 1: eccentricity = 0.06 m, and 2: eccentricity = 0.12 m, respectively.

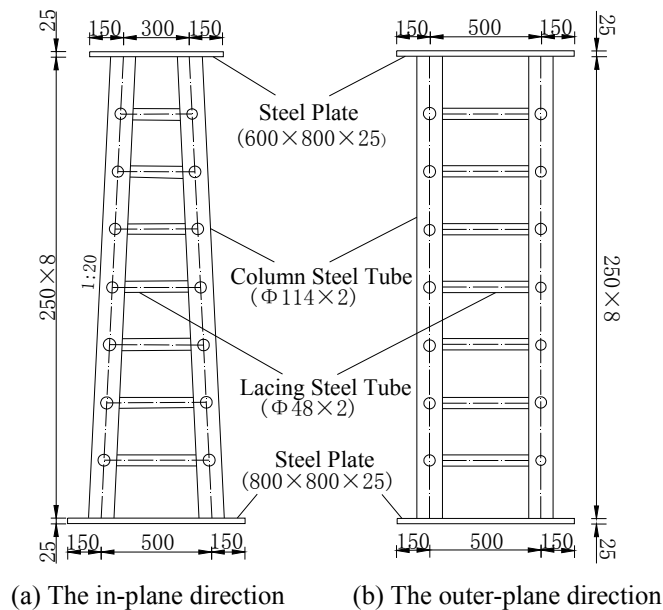


Fig. 1 Configuration of specimen PH1-2 (Unit: mm)

1:40; whereas that in the out-of-plane direction remains constant. Fig. 1 illustrates the configuration of specimen PH1-2. The section size is 500×500 mm and 300×500 mm for the bottom and the cap of the specimens with a slope of 1:20; and 400×500 mm and 300×500 mm for that with a slope of 1:40, respectively. The section size of uniform CFST latticed columns is the same as that of the cap of variable CFST latticed columns (300×500 mm). A triangle ribbed slab of 50×100×5 mm was welded to the steel plate.

The steel tubes are made of Q235 steel and filled with C40 concrete. The material properties of

Table 2 Material properties of specimens

Materials	Elastic modulus (105MPa)	Yield strength (MPa)	Ultimate strength (MPa)	Poisson ratio
Column steel tubes	2.05	300	444	0.27
Lacing steel tubes	1.98	351	488	0.28
Concrete	0.325	/	38	/

column steel tubes, lacing steel tubes, and concrete are shown in Table 2. In this experiment, 3 single CFST columns of the same batch were prepared, where the column height is 0.35 m and the average ultimate load-carrying capacity under axial compression is 580 kN.

2.2 Experimental procedures

Load was applied using a 500 T jack. The loading system consisted of upright column, cross beam, and base, and the upright column and cross beam comprised the reaction frame. Longitudinal and circumferential strain gages were placed at four points (A, B, C, and D in Fig. 2) at the 3/16, 9/16, and 13/16 cross sections of the specimens with a height of 2 m; whereas at the 1/4, 15/28 and 3/4 cross sections of the specimens with a height of 3.5 m, respectively. Longitudinal strain gages were placed at three points (E, F, and G in Fig. 2) at the upper margin of the 1/4, 1/2 and 3/4 cross sections of the lacing tubes. The arrangement of strain gages is schematically shown in Fig. 2. Displacement meters were placed at both ends of the columns to measure the longitudinal displacement, and several displacement meters were also placed along the columns in the in-plane direction to measure the lateral deflection.

The loading setup is shown in Fig. 3. Monotonic step loading was applied with an increment of 1/15 of the ultimate load in the initial loading phase. However, the increment was reduced to 1/20 of the ultimate load when the total load exceeded 50% of the ultimate load, and then further to 1/25 of the ultimate load when the total load exceeded 75% of the ultimate load. When the load reached the maximum value, loading continued for some time in order to obtain the stain and deflection of the specimens under ultimate loading conditions.

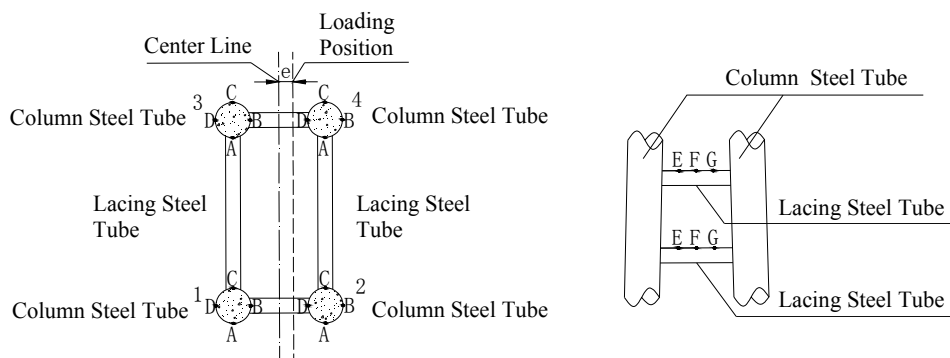


Fig. 2 The arrangement of strain gages



Fig. 3 Loading set-up

3. Experimental results and analysis

3.1 Load-carrying capacity of specimens

The experimental procedures are essentially the same for all the axial compression of specimens in this study. Take specimen PH1-2 as an example. Fig.4 shows the load-deflection curve of the specimen PH1-2 under axial compression, where the deflection refers to the lateral deflection at the middle section of the columns. It shows that the load-deflection curve of PH1-2 can be roughly classified into three phases, including elastic phase (OA), elastic-plastic phase (AB) and failure phase (BC). The specimen is initially in the elastic phase; and then column steel tubes gradually enter into a yield state at an applied load of 65-70% of the ultimate load, and the load-deflection curve deviates markedly from a straight line, indicating that the specimen is in the elastic-plastic phase. However, at an applied load of 93-95% of the ultimate load, the curve

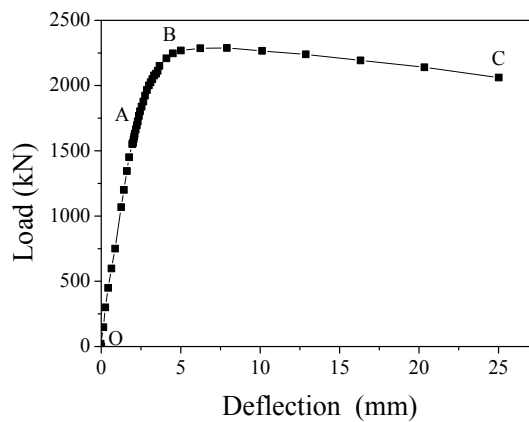
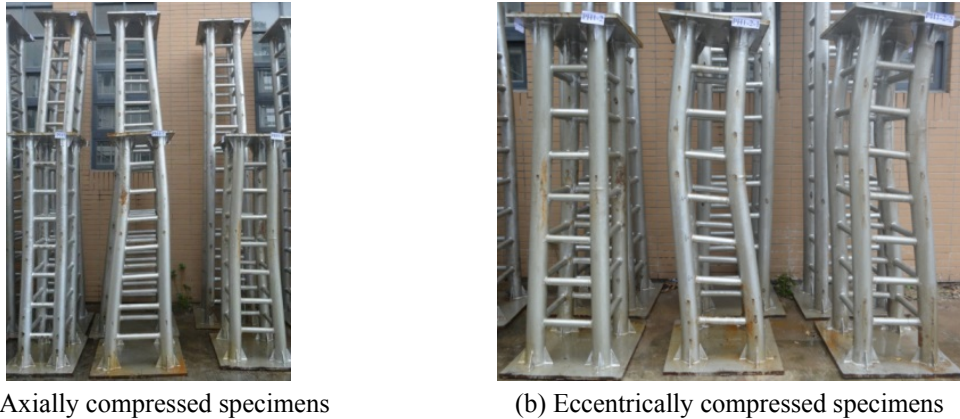


Fig. 4 Load-deflection curve of specimen PH1-2



(a) Axially compressed specimens

(b) Eccentrically compressed specimens

Fig. 5 Failure of axially and eccentrically compressed specimens

increases at a small rate, and in this case even a small increment in load can lead to an extremely large deflection. When the load cannot be further increased, the specimen deforms very rapidly and the load decreases slowly, indicating good ductility of the specimen. The peak load of the load-deflection curve is taken as the ultimate load-carrying capacity of the specimen in this experiment.

Lateral deformation is observed in the failure of axially compressed specimens because of the initial imperfection of the axially compressed specimens, installation deviation and error of eccentric loading. Fig. 5(a) shows the photos for the failure of axially compressed specimens. It is clear that all of these specimens exhibit an overall failure mode. Fig. 5(b) shows the failure of eccentrically compressed specimens. Variable CFST latticed columns show obvious in-plane bending under eccentric loading. As the eccentricity increases, the bending position at the loading side is closer to the column cap.

3.2 The effect of slope coefficient

Fig. 6 shows the load-deflection curves of axially compressed specimens with different slope coefficients (1:20 and 1:40), where deflection also refers to the lateral deflection at the middle cross section of the columns. These load-deflection curves can also be divided into elastic phase, elastic-plastic phase and failure phase. Due to the good ductility of CFST, the load reaches a maximum value and then decreases slowly. A close comparison of the load-deflection curves shows that for different variable CFST latticed columns of the same height, the larger the slope coefficient (1:n), the larger the slope of the load-deflection curves in the elastic phase, and consequently the larger the flexural rigidity. It is also important to note that higher specimens tend to have a more significant deflection.

Fig. 7 shows the ultimate load-carrying capacities of axially compressed specimens with different slope coefficients. The results clearly show that the ultimate load-carrying capacity of axially compressed variable CFST latticed columns is higher than that of uniform CFST latticed columns of the same height. The larger the slope coefficient (1:n), the larger the ultimate load-carrying capacity of variable CFST latticed columns under axial compression. For those 2-m specimens, the ultimate load-carrying capacity is increased by 3% and 5% for variable CFST latticed columns with a slope of 1:40 and 1:20 as compared with that of uniform CFST latticed

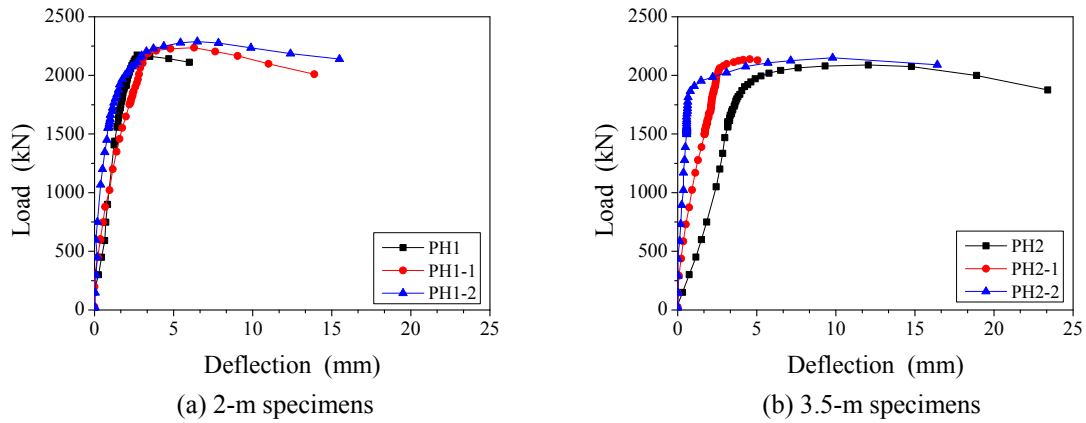


Fig. 6 Load-deflection curves for specimens with different slope coefficient

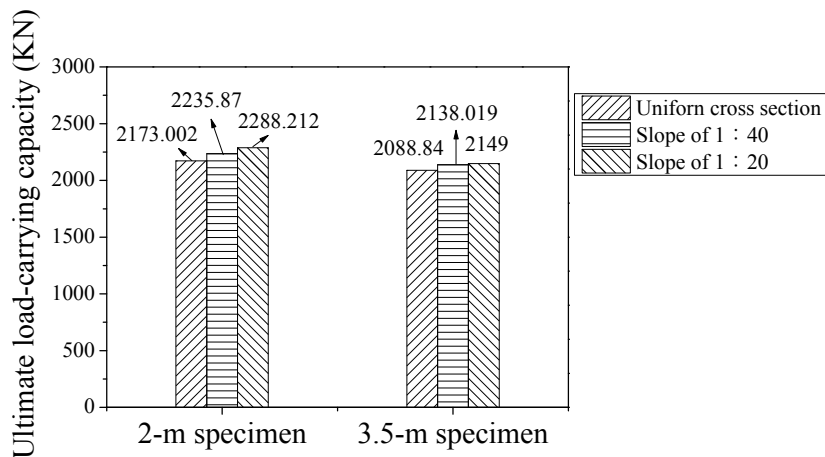


Fig. 7 Ultimate load-carrying capacity of axially compressed columns with different slope coefficients

columns, respectively. Given the same slope coefficient, the ultimate load-carrying capacity of axially compressed variable CFST latticed columns increases with decreasing slenderness ratio.

3.3 The effect of slenderness ratio

We also investigated the effect of slenderness ratio on the ultimate load-carrying capacity of variable CFST latticed columns. The slenderness ratio λ is defined as the ratio of the height of uniform CFST latticed columns to the radius of gyration of the cross section. In this study, the slenderness ratios of specimens of different heights are calculated by Eqs. (1) and (2) (Ou *et al.* 2011), and the results are shown in Table 1.

$$\lambda = l / i \tag{1}$$

$$i = \sqrt{(EI)_{sc} / (EA)_{sc}} \tag{2}$$

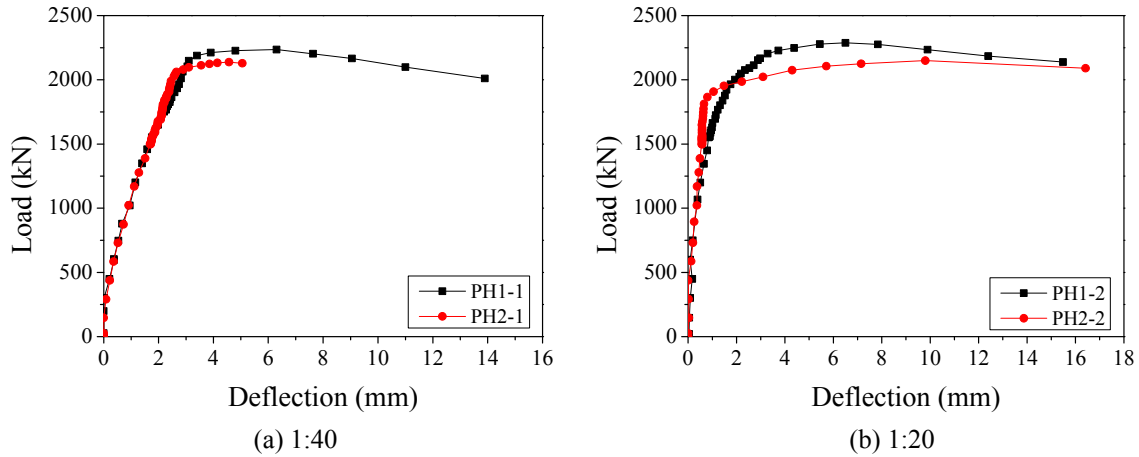


Fig. 8 Load-deflection curves for specimens with different slenderness ratios

Where $(EI)_{sc} = \sum E_s I_s + \sum E_c I_c$, $(EA)_{sc} = \sum E_s A_s + \sum E_c A_c$; E_s , E_c , I_s , I_c , A_s and A_c are the elasticity modulus, area and rigidity of the steel tube and concrete, respectively.

Fig. 8 shows the load-deflection curves of specimens with different slenderness ratios. It clearly shows that as there is only a marginal difference in the slenderness ratio between different specimens, the load-deflection curves almost coincide with each other in the elastic phase. However, in the latter loading phases, the slope of the curve is smaller for specimens with a larger slenderness ratio, and the corresponding ultimate load-carrying capacity decreases.

From Table 1, we can see that the ultimate load-carrying capacity of CFST latticed columns decreases with increasing slenderness ratio, which is in agreement with the results of previous studies (Ou *et al.* 2011). However, it is noted that the ultimate load-carrying capacity of variable CFST latticed columns is higher than that of uniform CFST latticed columns with the same height. As compared with the uniform CFST latticed columns with a slenderness ratio of 13, the ultimate load-carrying capacity is decreased by 4% and 6% for variable CFST latticed columns with a slope of 1:40 and 1:20, respectively.

3.4 The effect of eccentricity

Fig. 9 shows the deflection of variable CFST latticed columns with a height of 2 m and a slope coefficient of 1:40 under eccentric loading conditions, where deflection refers to the average deflection at the middle cross section of the two columns at the loading side. The load-deflection curves could also be roughly divided into three phases, including elastic phase, elastic-plastic phase and failure phase. As the load reaches 90-95% of the ultimate load, the whole specimen shows an obvious in-plane bending. Wrinkling is also observed at the top and a certain height of the steel tube at the loading side. Consequently, loading cannot be increased anymore and the pressure of the jack decreases, indicating the termination of the experiment.

It also can be seen from Table 1, the ultimate load-carrying capacity of eccentrically compressed columns decreases with the increase of eccentricity. As compared with the specimen PH1-1 under axial compression, the ultimate load-carrying capacity is decreased by 26.9% and 40.9% for the specimen PH1-1-1 with an eccentricity of $e_0 = 0.06$ m and the specimen PH1-1-2

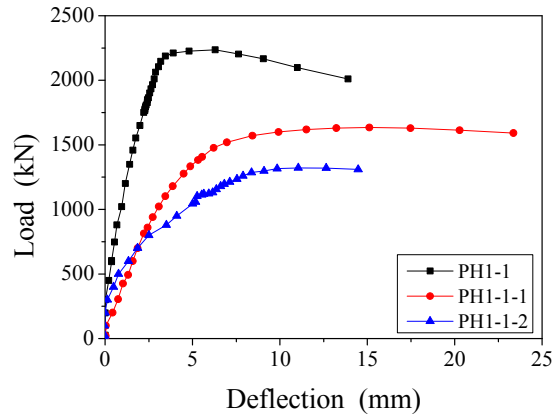


Fig. 9 Load- deflection curves for specimens with different eccentricities

with an eccentricity of $e_0 = 0.12$ m, respectively. In addition, the maximum deflection is observed at about 1/3 column height from the column cap of variable CFST latticed columns.

3.5 The confining effect of steel tubes

We investigated the confining effect of steel tubes on the concrete filled in the steel tubes based on the Poisson ratio of composite materials, which is defined as the absolute value of the ratio of the circumferential strain to the longitudinal strain of steel tubes. The experimental results show that the Poisson ratio of column steel tubes is 0.27 in the elastic phase. When the Poisson ratio of composite materials exceeds that of steel tubes, it is expected that steel tubes have a confining effect on the concrete. Fig. 10 shows the load-Poisson ratio curves for composite materials at point A at the middle cross section of No. 1 column under axial compression. In the initial loading stage, the Poisson ratio of composite materials is about 0.27, indicating a weak confining effect of steel tubes on the concrete. However, as the load is increased to 60-70% of the ultimate load, the Poisson ratio of composite materials exceeds 0.27 and increases very rapidly with increasing load, indicating that steel tubes have a significant effect on the concrete. A comparison between Figs. 10(a) and (b) shows that the Poisson ratio (0.47~0.55) of composite materials of the 3.5-m high specimens under ultimate loading condition is lower than that of the 2-m high specimen (0.57~0.72), indicating that the confining effect of steel tubes on the concrete under the ultimate loading conditions decreases with increasing slenderness ratio.

3.6 Load-carrying capacity of columns and lacing tubes

No failure is observed in the columns and lacing tubes prior to the total failure of specimens. The axial force carried by the columns can be described by the average longitudinal strain. Fig. 11(a) shows the average longitudinal strain at points A, B, C, and D at the middle cross section of the specimen PH1-1 under axial compression. The results show that in the elastic phase, the load-average longitudinal strain curves for the four columns almost coincide, indicating that the axial force is basically the same for the four columns. However, it is important to note that as the load increases, there is some difference in the average longitudinal strain between columns at the loading side (No. 2 and 4 columns) and columns at the opposite side (No.1 and 3 columns), which

can be attributed to the fact that the geometric nonlinearity of the specimens increases as the deflection increases, and columns are in small eccentric compression. Fig. 11(b) shows the load-average longitudinal strain curves at the 9l/16 cross section of the columns under eccentric compression. It clearly shows that the strain of steel tubes of No. 2 and No. 4 columns at the loading side is always higher than that of No. 1 and No. 3 columns at the opposite side. However, as the eccentricity increases, the difference in the average longitudinal strain between them increases. The load-longitudinal strain curves of columns at the loading side evolve into the nonlinear and reinforcement phase early, whereas that of columns at the opposite side are a straight line. The final failure of the specimens is caused by the failure of the columns at the loading side.

Fig. 12 shows the load-strain curve of the lacing tubes. It shows that the strain at the 1/4 cross section is very close to that at the 3/4 cross section, but with opposite signs. In the elastic phase of

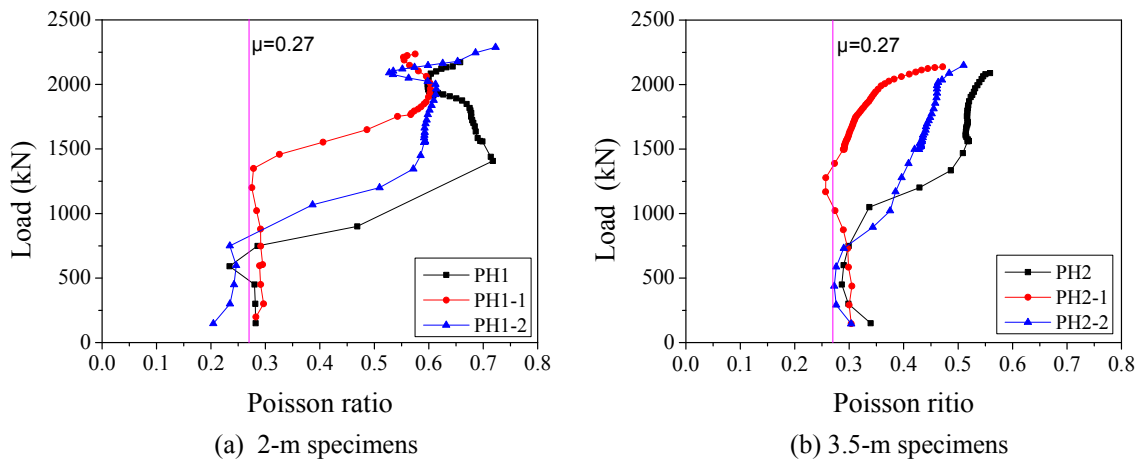


Fig. 10 Load-Poisson ratio curves of composite materials of specimens under axial compression

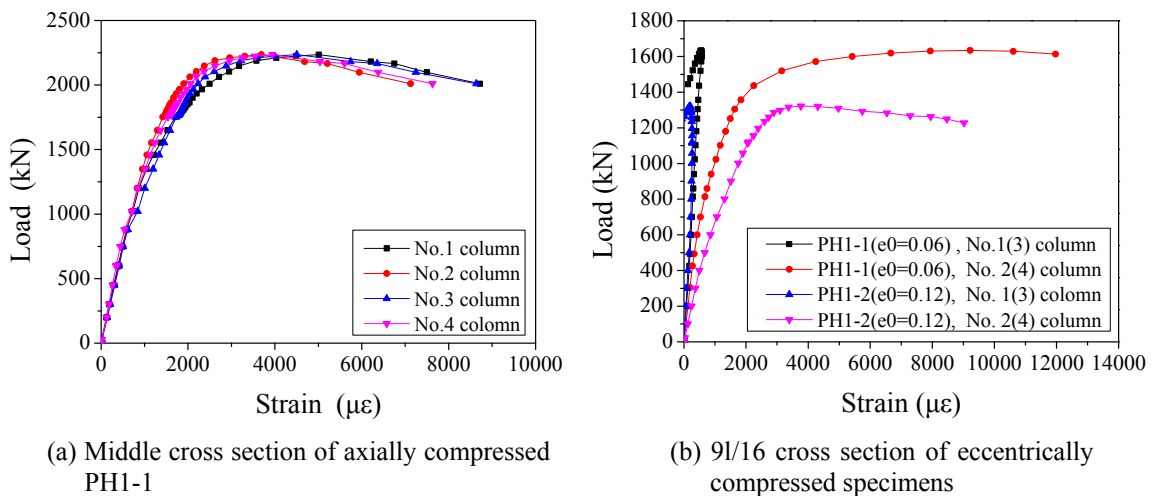


Fig. 11 Load-average longitudinal strain curves of the four columns

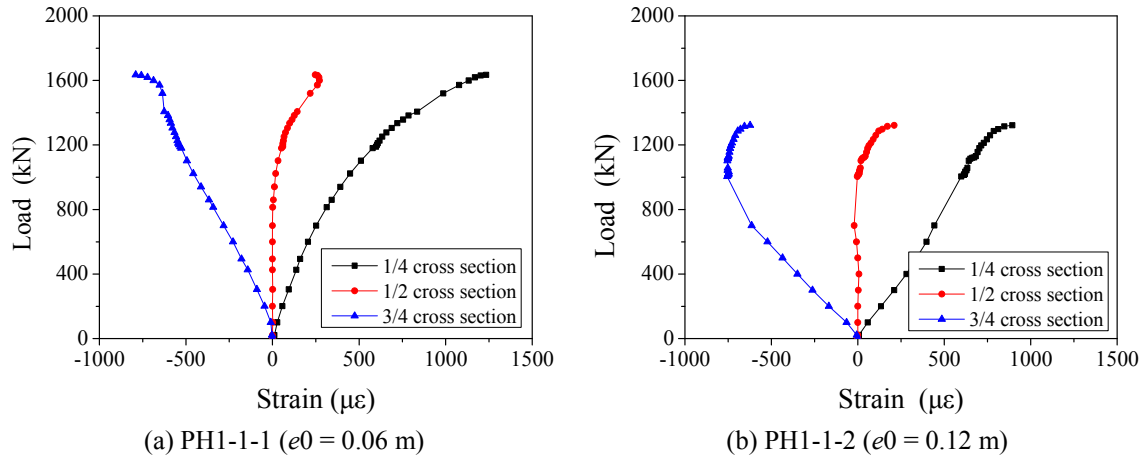


Fig. 12 Load-deformation curves of middle lacing tubes

the whole latticed columns, the strain at the 1/2 cross section is close to 0, and the lacing tubes basically show S-shaped deformation. The yield strain of lacing tubes is $1773 \mu\epsilon$. A close comparison between Figs. 12(a) and (b) shows that as the eccentricity increases, the strain of lacing tubes increases rapidly, but the maximum strain is always smaller than the yield strain, thus indicating that the lacing tubes are basically in the elastic phase.

4. Conclusions

Some important conclusions can be drawn from these results.

- All the variable CFST latticed columns show an overall failure under axial compression, which is similar to that of uniform CFST latticed columns. However, the flexural rigidity of variable CFST latticed columns is higher than that of uniform CFST latticed columns, and the larger the slope coefficient, the larger the flexural rigidity.
- Under eccentric compression, the maximum deflection is observed at about 1/3 column height from the cap of the variable CFST latticed columns. For the variable CFST latticed columns, the strain of the columns at the loading side, as well as the difference in the strain, increases from the bottom to the cap, and a more significant increase in strain is observed in the cross section closer to the column cap. In addition, the ultimate load-carrying capacity of variable CFST latticed columns decreases as the eccentricity increases.
- The ultimate load-carrying capacity of variable CFST latticed columns under axial compression is higher than that of uniform CFST latticed columns of the same height. The larger the slope coefficient, the larger the ultimate load-carrying capacity of variable CFST latticed columns under axial compression. For those 2-m specimens, the ultimate load-carrying capacity is increased by 3% and 5% for variable CFST latticed columns with a slope of 1:40 and 1:20 as compared with that of uniform CFST latticed columns, respectively. As compared with the uniform CFST latticed columns with a slenderness ratio of 13, the ultimate load-carrying capacity is decreased by 4% and 6% for variable CFST latticed columns with a slope of 1:40 and 1:20, respectively.

Acknowledgments

The authors would like to express their sincere gratitude to the National Natural Science Foundation of China (No. 51578156) and the foreign cooperation projects of science and technology agency in Fujian Province (No. 2015I0012) for providing the necessary funds for this research work.

References

- An, Y.F., Han, L.H. and Zhao, X.L. (2012), "Behavior and design calculations on very slender thin-walled CFST columns", *Thin-Wall. Struct.*, **53**, 161-175.
- Banan, M.R. and Fouladi, A. (2015), "A super-element based on finite element method for latticed columns", *Int. J. Civil Eng.*, **13**(2), 202-212.
- Bleich, F. (1952), *Buckling Strength of Metal Structures*, McGraw-Hill Book Company, New York, NY, USA.
- CECS 28: 90 (2012), Specification for design and construction of concrete filled steel tubular structures, Harbin Jianzhu University and China Academy of Building Research, Harbin, China. [In Chinese]
- Chen, B.C. (2002), *Examples of Concrete Filled Steel Tubular Arch Bridges (One)*, Communications Press, Beijing, China. [In Chinese]
- Cristutiu, I.M. and Dogariu, A.I. (2012), "The behaviour of beam-column elements with variable I cross-sections considering lateral restraints", *Proceedings of the 11th International Conference on Computational Structures Technology*, Dubrovnik, Croatia, September, pp. 1-15.
- Dai, S.J., Yang, L. and Jia, Y.H. (2013), "A study on the formulas of effective slenderness ratio of three-legged lattice column", *Appl. Mech. Mater.*, **405-408**, 940-943.
- Han, L.H., He, S.H. and Liao, F.Y. (2011), "Performance and calculations of concrete filled steel tubes (CFST) under axial tension", *J. Construct. Steel Res.*, **67**(11), 1699-1709.
- Jiang, L.Z., Zhou, W.B. and Qi, J.J. (2011), "Numerical method and experimental study on the ultimate load carrying capacity of four-tube CFST latticed columns", *J. Adv. Mater. Res.*, **163-167**, 2224-2233.
- Lee, G.C., Ketter, R.L. and Hsu, T.L. (1981), "The design of single story rigid frames", *Metal Building Manufacture's Association*, Cleveland, OH, USA.
- Li, J.J. and Li, G.Q. (2004), "Buckling analysis of tapered lattice columns using a generalized finite element", *Commun. Numer. Method. Eng.*, **20**(6), 479-488.
- Mijailovic, R. (2010), "Optimum design of lattice-columns for buckling", *J. Struct. Multidiscipl. Optimiz.*, **42**(6), 897-906.
- Mohri, F., Damil, N. and Potier-Ferry, M. (2013), "Buckling and lateral buckling interaction in thin-walled beam-column elements with mono-symmetric cross sections", *Appl. Math. Model.*, **37**(5), 3526-3540.
- Ou, Z.J., Chen, B.C., Hsieh, K.H., Halling, M.W. and Barr, P.J. (2011), "Experimental and analytical investigation of concrete filled steel tubular columns", *J. Struct. Eng.*, **137**(6), 635-645.
- Pual, M. (1995), "Buckling loads of built-up columns with stay plates", *ASCE, J. Eng. Mech.*, **121**(11), 1200-1208.
- Qu, X.S., Chen, Z.H. and Sun, G.J. (2015), "Axial behavior of rectangular concrete-filled cold-formed steel tubular columns with different loading methods", *Steel Compos. Struct., Int. J.*, **8**(1), 71-90.
- Razdolsky, A.G. (2011), "Calculation of slenderness ratio for laced columns with serpentine and crosswise lattices", *J. Construct. Steel Res.*, **67**(1), 25-29.
- Samofalov, M. and Šlivinskas, T. (2009), "Stability analysis of steel frames with variable cross-section for sports and entertainment centre", *MECHANIKA*, **5**(79), 5-12.
- Shi, L.Y., Li, Z.B. and Zhang, Z.Y. (2012), "The experimental research on the vertical and horizontal bearing capacity of hollow latticed steel columns", *Adv. Mater. Res.*, **461**, 425-428.
- Xue, J.Y., Gao L., Liu, Z.Q., Zhao, H.T. and Chen, Z.P. (2014), "Experimental study on mechanical

performances of lattice steel reinforced concrete inner frame with irregular section columns”, *Steel Compos. Struct., Int. J.*, **16**(3), 253-267.

CC